LETTERS

North Atlantic Atmosphere–Ocean Interaction on Intraseasonal Time Scales

LAURA M. CIASTO AND DAVID W. J. THOMPSON

Department of Atmospheric Science, Colorado State University, Fort Collins, Colorado

24 September 2003 and 14 November 2003

ABSTRACT

The authors examine wintertime atmosphere–ocean interaction on weekly time scales over the North Atlantic sector. Consistent with previous results, it is found that the strongest interactions between the ocean and atmosphere occur when the atmosphere leads. However, the authors also find a spatially coherent and statistically significant pattern of sea surface temperature anomalies over the Gulf Stream extension region that precedes changes in the leading mode of Northern Hemisphere atmospheric variablilty by ~2 weeks.

A substantial fraction of midlatitude sea surface temperature (SST) variability on time scales ranging from months (Frankignoul and Hasselman 1977) to years (Deser et al. 2003) can be interpreted as the passive thermodynamic response of the ocean mixed layer to stochastic atmospheric forcing. Subsequently, the dominant structures of monthly and seasonal mean Northern Hemisphere (NH) SST variability owe their existence to variations in the dominant patterns of variability in the midlatitude atmosphere (Bjerknes 1964; Wallace et al. 1990; Cayan 1992; Visbeck et al. 2003).

To what extent midlatitude SST variability, in turn, gives rise to anomalies in the dominant structures of midlatitude atmospheric variability remains unclear. General circulation models run with prescribed SST anomalies suggest that the amplitude of the extratropical atmospheric response to realistic midlatitude SST anomalies is modest compared to internal atmospheric variability (e.g., see the recent review by Kushnir et al. 2002). Hindcast experiments run with prescribed global SSTs closely reproduce observed atmospheric variability (Rodwell et al. 1999; Mehta et al. 2000), but the results do not prove a robust dynamic response of the extratropical atmosphere to midlatitude SST anomalies (Bretherton and Battisti 2000). Observational studies based on temporally and spatially dense satellite data imply that extratropical SSTs give rise to changes in the overlying surface winds (O'Neill et al. 2003; Nonaka and Xie 2003), but it is unclear to what extent this effect extends above the boundary layer. Recent observational analyses based on lagged monthly mean data suggest that summertime SST anomalies yield predictive skill for wintertime climate (Czaja and Frankignoul 1999), but the correlations are restricted to a small fraction of the NH winter (Kushnir et al. 2002).

Presumably, if the extratropical atmosphere exhibits a deep and statistically significant response to midlatitude SST anomalies, the dynamics of the response should occur on time scales shorter than the monthly and seasonal means used in most observational analyses of extratropical atmosphere–ocean interaction. With this in mind, Deser and Timlin (1997, hereafter DT) investigated large-scale NH atmosphere–ocean interaction using 14 yr of weekly mean data. Based on the results of lagged singular value decomposition (SVD) analysis between standardized values of SST and 500-hPa height, DT concluded that the dominant patterns of NH atmospheric variability lead variations in the SST field by 2–3 weeks, but they did not focus on any patterns in the SST field that, in turn, lead atmospheric variability. In this letter, we revisit the analysis of DT, but more closely examine the lead–lag relationships between North Atlantic SST anomalies and the dominant pattern of Northern Hemisphere variability, the so-called Northern Hemisphere annular mode (NAM; also referred to as the North Atlantic Oscillation and Arctic Oscillation).

We use 22 yr (1981–2002) of weekly mean SST data described in Reynolds et al. (2002) and weekly averages of sea level pressure (SLP) and zonal-wind data from the National Centers for Environment Prediction–National Center for Atmospheric Research (NCEP–NCAR) Reanalysis Project (Kalnay et al. 1996). The SST data

Corresponding author address: Laura M. Ciasto, Department of Atmospheric Science, Colorado State University, Fort Collins, CO 80523-1371.
E-mail: lciasto@atmos.colostate.edu

are available on a 1° × 1° latitude–longitude grid and were smoothed with a three-point binomial filter applied in both space and time, as per discussions in O'Neill et al. (2003) and Reynolds et al. (2002). Results are based on the 23-week winter season extending from the first week in November to the last week in March, and lag regressions are centered about the months December–February. We remove the seasonal cycle and we also remove each winter's mean from the weekly data for that winter (the anomalous intraseasonal SST data are hereafter denoted SST_{is}). By removing each winter's mean, we isolate processes that occur on subseasonal time scales from those that occur on interannual and longer time scales. Note that the removal of the winter–winter variability does not impact the asymmetry of the lag regressions on intraseasonal time scales. The statistical significance of all correlation coefficients is assessed using the *t* statistic in which the effective sample size is estimated using the relationship outlined in Bretherton et al. [1999, their Eq. (31)]. In the case of correlations between SLP and SST, the 95% confidence level is $r \sim 0.25$; for correlations between SST and atmospheric tendency, it is $r \sim 0.20$.

Figure 1 shows the regression of SST_{is} onto the standardized time series of the NAM at lags ranging from −4 to +4 weeks. Weekly values of the NAM index were formed by averaging daily values of the NAM index described in Thompson and Wallace (2001). By convention, the NAM index is standardized and positive values denote lower-than-normal geopotential heights over the pole, and vice versa. At positive lags (ocean lagging), the regression maps are marked by SST anomalies that are significantly lower than normal to the south of Greenland, higher than normal over the region extending eastward from the coast of the United States, and lower than normal in the subtropical North Atlantic. Significantly higher SST anomalies are also observed along the coast of northwestern Europe. The meridionally banded structure evidenced in Figs. 1d,e is commonly referred to as the ''tripole'' in North Atlantic SSTs and is linked to the anomalous surface fluxes of sensible and latent heat associated with the NAM (Cayan 1992; Visbeck et al. 2003).

At negative lags (ocean leading), a different pattern in SST emerges. In contrast to the pattern evident in Fig. 1d, the regression maps in Figs. 1a,b have the largest amplitude along the Gulf Stream extension, near the subpolar node of the tripole. The largest and most significant SST anomalies in the Gulf Stream extension region occur ~2 weeks prior to the peak in the NAM and have an amplitude comparable to that observed in the subpolar center of the tripole (~0.25°C). A similar pattern is also evident in DT (their Fig. 1a), but this feature is not highlighted in their SVD analysis of standardized data.

Expansion coefficient time series of the Gulf Stream extension pattern in Fig. 1b (referred to hereafter as G) and the tripole pattern in Fig. 1d were formed by pro-

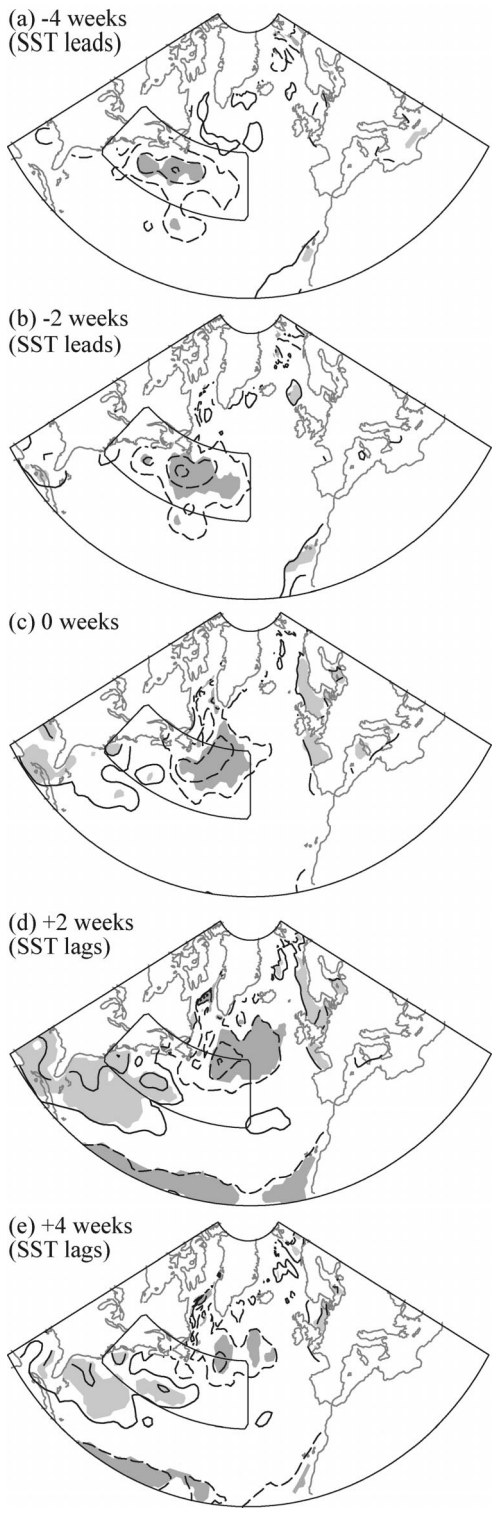

FIG. 1. Weekly wintertime intraseasonal SST anomalies regressed on the NAM index at (a) lag −4 weeks (SST leads NAM), (b) lag −2 weeks, (c) lag 0 weeks, (d) lag +2 weeks (SST lags NAM), (e) lag +4 weeks. Positive (negative) contours are denoted by solid (dashed) lines and are drawn at −0.05°, 0.05°, 0.15°C, . . . , etc. Areas that exceed the 95% confidence level ($r \sim 0.25$) are shaded. The box denotes the region 35°–50°N, 30°–75°W.

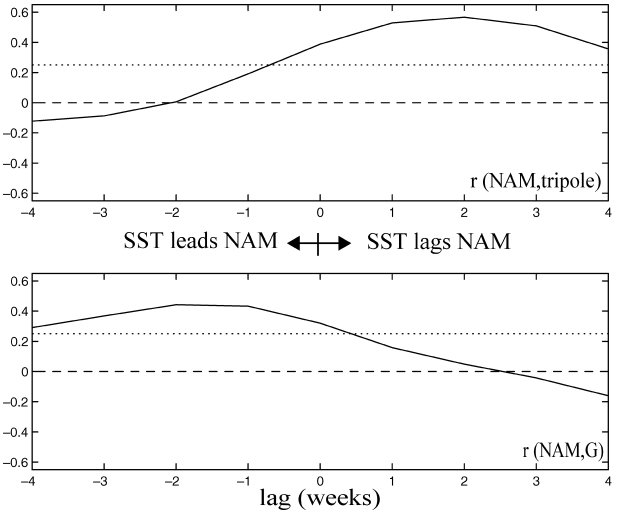

FIG. 2. Lag correlation coefficients (solid line) between weekly wintertime intraseasonal values of the NAM index and the expansion coefficient time series of the patterns in (top) Fig. 1d and (bottom) Fig. 1b. The 95% confidence level is denoted by the dotted line.

jecting the respective regression maps onto the SST_{is} data. In practice, the corresponding time series for G is highly correlated with SST anomalies averaged over the box indicated in Fig. 1 ($r = -0.91$). Consistent with the results presented in DT, the lag correlations between the NAM and the tripole (Fig. 2, top) are largest and most significant when the NAM leads by ~2–3 weeks. The attendant asymmetry in the lag correlations implies that variability in the NAM gives rise to variations in the tripole, but not vice versa. In contrast, the lag correlations between the NAM and G (Fig. 2, bottom) are largest and most significant when G leads by 1–2 weeks, and drop to near zero at positive lags. The asymmetry in the lag correlations between the NAM and G implies that changes in SSTs over the Gulf Stream extension region tend to precede changes in the NAM on intraseasonal time scales.

If SST anomalies in the Gulf Stream extension region are associated with changes in the overlying atmospheric circulation, the relationships should be evident in the regression of the tendency of various atmospheric parameters onto contemporaneous values of G. Figure 3 shows the regression of the tendency in SLP (bottom) and the zonal-mean zonal wind (top) onto standardized values of G. The tendency is defined as the difference in data between +2 and −2 weeks; in practice, qualitatively similar results are derived for tendencies defined as the difference in data between +3 and −3 and between +4 and −4 weeks, and when the basis of the regression is defined as SST anomalies averaged over the box indicated in Fig. 1. The tendency regression maps in Fig. 3 bear evident similarity to the NAM: positive values of G (i.e., lower-than-normal SSTs over the Gulf Stream extension) are characterized by falling pressures over the Arctic/subpolar North Atlantic juxtaposed against rising pressures over the central North Atlantic and North Pacific, and by an equivalent barotropic strengthening of the westerly flow along ~55°N. The results in Fig. 3 are dominated by the atmosphere-lagging component of the tendency (not shown), and thus reflect increasing amplitude of the NAM with time. In contrast, analogous results based on the time series of the tripole are dominated by the atmosphere-leading component of the tendency (not shown), and thus reflect decreasing amplitude of the NAM with time.

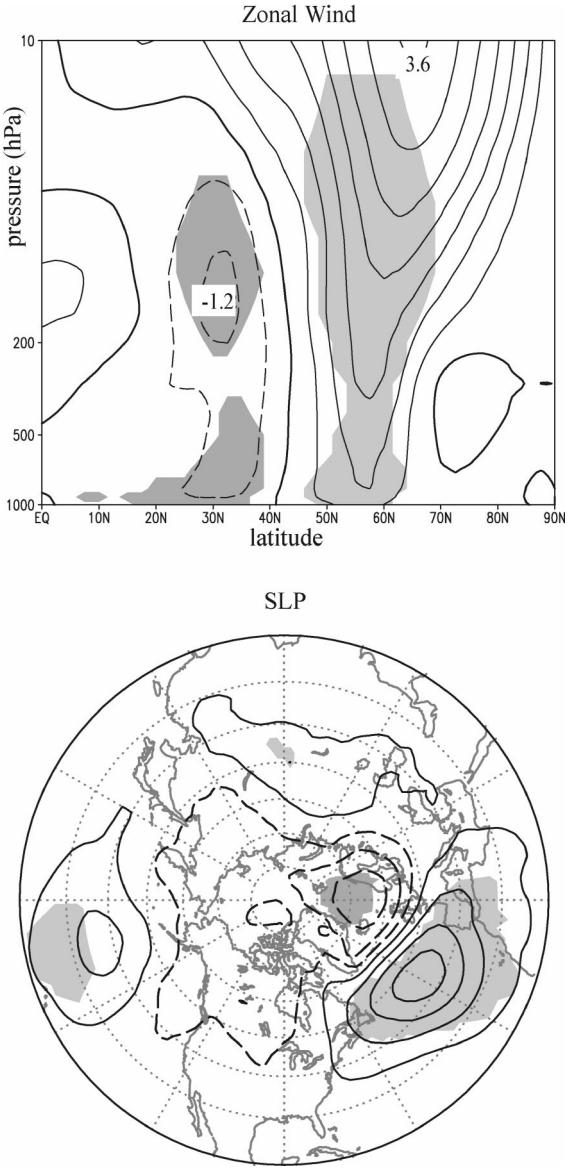

FIG. 3. The tendency in intraseasonal wintertime values of the (top) zonal-mean zonal wind and (bottom) SLP (expressed as Z_{1000}) regressed on the expansion coefficient time series of the pattern in Fig. 1b. The tendency is defined as the difference in data between +2 and −2 weeks. Contours are at (top) −0.5, 0, 0.5 m s^{-1} . . . , etc., and (bottom) −5, 5, 15 m . . . , etc. Positive (negative) contours are denoted by solid (dashed) lines. Areas that exceed the 95% confidence level ($r \sim 0.20$) are shaded.

The results in Figs. 1–3 support the conclusion reached by DT that on subseasonal time scales the strongest covariability between the extratropical atmosphere and ocean occurs when the atmosphere leads by ~2 weeks. But the results also demonstrate a distinct and statistically significant pattern of SST variability over the Gulf Stream extension region that precedes changes in the leading mode of NH atmospheric variability. This pattern is hinted at in DT, but is not accentuated in their SVD analysis of 14 yr of standardized data. The correlations between G and the NAM exceed the 95% significance level when the ocean leads by 2 weeks, and the asymmetry in the lag correlations revealed in Fig. 2 (bottom) is evident in more than 95% of 500 randomized subsamples of the data consisting of 10 randomly chosen winters each.

The center of action of G is located within a zone of pronounced gradients in SSTs and corresponds to the region of largest intraseasonal variability in the North Atlantic (Fig. 4a). On the time scales considered in this study, variations in G arise from anomalies in the fluxes of latent and sensible heat at the ocean surface, with possible contributions from mesoscale ocean eddies, mean advection by ocean currents, and anomalous Ekman currents. Potential explanations for the relationships observed in this study include:

1) *Variations in G reflect forcing by the NAM at a previous lag.*
   If variations in G reflect forcing by the NAM at a previous lag, the structure of atmospheric circulation anomalies associated with increasing amplitude in G should resemble the structure of the NAM at an earlier stage in its life cycle. The results in Figs. 4b,c reveal that this is not the case. The pattern of SLP anomalies that precedes peak amplitude in G by 2 weeks is characterized by anomalously low SLP centered between ~55°N and 35°W, consistent with anomalous cold advection in the vicinity of the Gulf Stream extension (Fig. 4b). In contrast, the pattern of SLP anomalies that precedes peak amplitude in the NAM by 4 weeks (and hence by inference, precedes peak amplitude in G by 2 weeks) projects only weakly onto the surface circulation in regions where G has largest amplitude (Fig. 4c).

2) *Variations in G give rise to variations in the NAM.* That atmospheric variability contributes to intraseasonal variations in SST over the Gulf Stream extension does not preclude SSTs in this region from providing a feedback to the atmospheric circulation. Variations in G underlie a region of marked cyclogenesis over the western edge of the North Atlantic storm track. Thus, the anomalous surface heat fluxes that must accompany G as it decays on weekly time scales are uniquely positioned to perturb the extratropical atmosphere. Lower-than-normal SSTs in the Gulf Stream extension will tend to shift the region of largest SST gradient equatorward, but will also tend to weaken the temperature contrast between the continent and ocean. The latter effect would be expected to suppress the growth of baroclinic eddies off the east coast of North America, and hence potentially lead to enhanced growth and amplitude in the northeast Atlantic consistent with the tendency regressions in Fig. 3 (B. J. Hoskins 2003, personal communication).

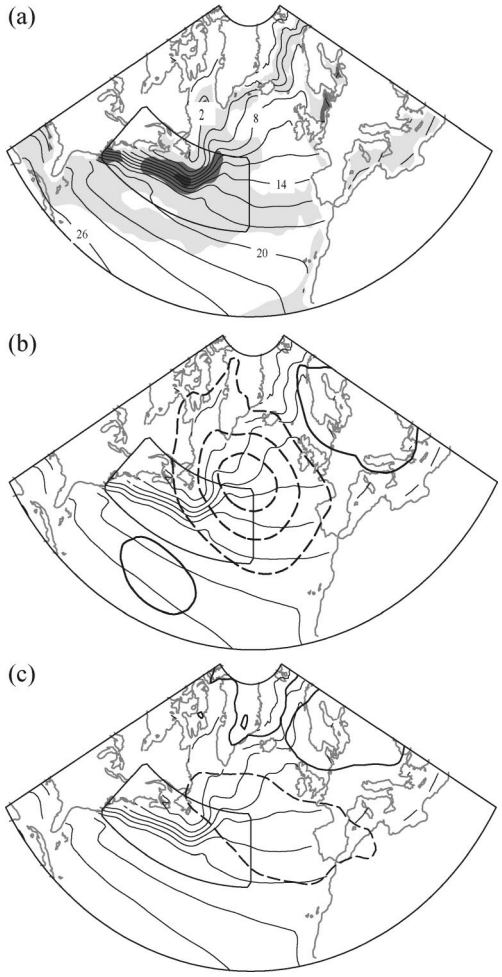

FIG. 4. Nov–Mar climatological mean SSTs (thin contours) and (a) the std dev of intraseasonal Nov–Mar SST anomalies (shading at 0.3°, 0.6°, 0.9°C); (b) wintertime SLP anomalies regressed onto time series of G when SLP leads by 2 weeks (thick contours); and (c) wintertime SLP anomalies regressed onto NAM when SLP leads by 4 weeks (thick contours). SLP (expressed as Z_{1000}) contours are at −5, 5, 15 m . . . , etc. Positive (negative) contours are denoted by solid (dashed) lines. The box denotes the region 35°–50°N, 30°–75°W.

An obvious caveat to the latter mechanism is the amplitude of the associated atmospheric and SST anomalies. A typical ~0.5-K fluctuation in SST over the Gulf Stream extension region projects only weakly onto the climatological SST gradient there (Fig. 4a), and the largest anomalies in Figs. 1b and 3 account for only ~20% of the total variance in their respective fields. Another caveat is the inconsistency of the general circulation

model (GCM) response to midlatitude SST anomalies. Palmer and Sun (1985), Ferranti et al. (1994), and Peng et al. (1995) all examine the GCM response to a pattern of SST anomalies reminiscent of G, but the amplitude and structure of the simulated responses varies not only from model to model, but from season to season as well (Peng et al. 1995; Kushnir et al. 2002). In light of these caveats, we are hesitant to conclude that the results in this study reveal that the NAM is responding to variations in SST over the Gulf Stream extension. However, it is equally difficult to interpret the tendency toward increasing amplitude of the NAM in Fig. 3 as the response of the ocean to atmospheric forcing.

Acknowledgments. We thank D. Battisti, A. Czaja, C. Deser, B. J. Hoskins, J. Hurrell, Y. Kushnir, and W. Robinson for their comments at various stages of this research. D. W. J. T. and L. M. C. are supported by the NSF under Grants ATM-0320959 and CAREER: ATM-0132190. We also thank T. Vonder-Haar at NOAA/CIRA for additional financial support.

REFERENCES

Bjerknes, J., 1964: Atlantic air-sea interaction. *Advances in Geophysics*, Vol. 10, Academic Press, 1–82.

Bretherton, C. S., and D. Battisti, 2000: An interpretation of the results from atmospheric general circulation models forced by the history of observed sea surface temperature distribution. *Geophys. Res. Lett.,* **27,** 767–770.

——, M. Widmann, V. P. Dymnikov, J. M. Wallace, and I. Bladé, 1999: The effective number of spatial degrees of freedom of a time-varying field. *J. Climate,* **12,** 1990–2009.

Cayan, D. R., 1992: Latent and sensible heat flux anomalies over the northern oceans: Driving the sea surface temperature. *J. Phys. Oceanogr.,* **22,** 859–881.

Czaja, A., and C. Frankignoul, 1999: Influence of the North Atlantic SST on the atmospheric circulation. *Geophys. Res. Lett.,* **26,** 2969–2972.

Deser, C., and M. S. Timlin, 1997: Atmosphere–ocean interaction on weekly timescales in the North Atlantic and Pacific. *J. Climate,* **10,** 393–408.

——, M. A. Alexander, and M. S. Timlin, 2003: Understanding the persistence of sea surface temperature anomalies in midlatitudes. *J. Climate,* **16,** 57–72.

Ferranti, L., F. Molteni, and T. N. Palmer, 1994: Impact of localized tropical and extratropical SST anomalies in ensembles of seasonal GCM integrations. *Quart. J. Roy. Meteor. Soc.,* **120,** 1613–1645.

Frankignoul, C., and K. Hasselman, 1977: Stochastic climate models. Part II: Application to sea-surface temperature variability and thermocline variability. *Tellus,* **29,** 289–305.

Kalnay, E., and Coauthors, 1996: The NCEP/NCAR 40-Year Reanalysis Project. *Bull. Amer. Meteor. Soc.,* **77,** 437–471.

Kushnir, Y., W. A. Robinson, I. Blade, N. M. J. Hall, S. Peng, and R. Sutton, 2002: Atmospheric GCM response to extratropical SST anomalies: Synthesis and evaluation. *J. Climate,* **15,** 2233–2256.

Mehta, V. M., M. J. Suarez, J. Manganello, and T. L. Delworth, 2000: Predictability of multiyear to decadal variations in the North Atlantic Oscillation and associated Northern Hemisphere climate variations: 1959–1993. *Geophys. Res. Lett.,* **27,** 121–124.

Nonaka, M., and S. P. Xie, 2003: Covariations of sea surface temperature and wind over the Kuroshio and its extension: Evidence for ocean–atmosphere feedback. *J. Climate,* **16,** 1404–1413.

O'Neill, L. W., D. B. Chelton, and S. K. Esbensen, 2003: Observations of SST-induced perturbations of the wind stress field over the Southern Ocean on seasonal timescales. *J. Climate,* **16,** 2340–2354.

Palmer, T. N., and Z. Sun, 1985: A modelling and observational study of the relationship between sea surface temperatures in the northwest Atlantic and the atmospheric general circulation. *Quart. J. Roy. Meteor. Soc.,* **111,** 947–975.

Peng, S., A. Mysak, H. Ritchie, J. Derome, and B. Dugas, 1995: The difference between early and middle winter atmospheric response to sea surface temperature anomalies in the northwest Atlantic. *J. Climate,* **8,** 137–157.

Reynolds, R. W., N. A. Rayner, T. M. Smith, D. C. Stokes, and W. Wang, 2002: An improved in situ and satellite SST analysis for climate. *J. Climate,* **15,** 1609–1625.

Rodwell, M. J., D. P. Rowell, and C. K. Folland, 1999: Ocean forcing of the wintertime North Atlantic oscillation and European climate. *Nature,* **398,** 320–323.

Thompson, D. W. J., and J. M. Wallace, 2001: Regional impacts of the Northern Hemisphere Annular Mode. *Science,* **293,** 85–89.

Wallace, J. M., C. Smith, and Q. Jiang, 1990: Spatial patterns of atmosphere–ocean interaction in the northern winter. *J. Climate,* **3,** 990–998.

Visbeck, M., E. P. Chassignet, R. G. Curry, T. L. Delworth, R. R. Dickson, and G. Krahmann, 2003: The ocean's response to North Atlantic Oscillation variability. *The North Atlantic Oscillation: Climate Significance and Environmental Impact,* J. W. Hurrell et al., Eds., Amer. Geophys. Union, 113–146.